

Fabrication and Characterization of Gold Nanoparticles by Femtosecond Laser Ablation in an Aqueous Solution of Cyclodextrins

Andrei V. Kabashin,[†] Michel Meunier,[†] Christopher Kingston,[‡] and John H. T. Luong^{*,§}

Laser Processing Laboratory, Department of Engineering Physics, Ecole Polytechnique de Montreal, Montreal, Quebec, Canada H3C 3A7; Steacie Institute of Molecular Sciences, National Research Council Canada, Ottawa, Ontario, Canada K1A 0R6; and Biotechnology Research Institute, National Research Council Canada, Montreal, Quebec, Canada H4P 2R2

Received: February 10, 2003

Gold nanoparticles were produced by femtosecond laser ablation of a gold metal plate in an aqueous solution of α -cyclodextrin (CD), β -CD, or γ -CD. The gold nanoparticles exhibited the UV–vis absorption spectrum with a maximum absorption band at 520 nm, similar to that of gold nanoparticles chemically prepared in a solution. The size distribution of the nanoparticles measured by transmission electron microscopy (TEM) shifted to a drastically smaller size of ~ 2 – 2.4 nm and narrower size distribution of less than 1 – 1.5 nm fwhm with an increase in the concentration of cyclodextrins. Both the particle size and size distribution were also dependent on the type of cyclodextrins used in aqueous solution. In particular, the gold colloids resulting from ablation in 10 mM β -CD were conspicuously stable under aerobic conditions without any protective agent present. CDs formed an inclusion complex with ablated atoms to reduce the total concentration of embryonic nanoparticles formed in the plume CDs, as evident by Raman spectroscopy. The consecutive particle growth due to the mutual coalescence between nanoclusters and their neighboring free gold atoms was severely limited in the presence of CDs.

Introduction

Nanomaterials with size-dependent physical properties provide great opportunities for a plethora of novel applications.¹ Among metal nanoparticles, gold nanoparticles possess several appealing features that make them very attractive for intensive research in nanotechnology. For instance, gold nanoparticles with diameters of 3 – 5 nm show a drastic decrease of the melting point,^{2a,b} and TiO₂-supported gold nanoparticles display a highly selective catalytic activity for CO oxidation at -70 °C.^{2c} To exploit the size and quantum confinement effects of nanoparticles and to tailor nanomaterials with new properties, it is of utmost importance to prepare monodispersed nanoparticles with a very narrow size distribution. Wet chemistry techniques have been overwhelmingly used to prepare gold nanoparticles in the 10 – 20 nm diameter range by the reduction of a diluted metal salt in aqueous solution with a reducing reagent.³ The preparation in a micelle or reverse micelle is one of the most successful methods to obtain metal nanoparticles stabilized in solutions.⁴ Alternatively, nanosecond laser ablation of a metal surface immersed in a liquid has also been known to produce metal nanoparticles in the liquid.⁵ However, the size distribution of the nanoparticles tends to be broadened, as both postablation particle agglomeration and the ejection of large melted fragments from the target usually take place because of the target Joule heating during the nanosecond laser ablation.⁶ Several attempts have been made for the size control by combining laser ablation with laser-induced size control, and the preparation is performed in an aqueous solution of surfactant such as sodium dodecyl sulfate (SDS).⁷

In this paper, we present another method to prepare stable nanoparticles by laser ablation of a metal plate in solutions containing neutral α -cyclodextrin (CD), β -CD, or γ -CD. CDs are toruslike macrocycles built up from D-(+)-glucopyranose units, which are linked by α -1–4-linkages (the most common ones are α -, β -, and γ -CDs, consisting of six, seven, and eight units, respectively).⁸

Experimental Section

Materials and Chemicals. α -Cyclodextrin (α -CD), β -CD, and γ -CD were obtained from Sigma-Aldrich (St. Louis, MO) and used without further purification. All solutions were prepared from high-purity deionized water. CD solutions were prepared as stock solutions in appropriate buffers immediately prior to their use. A gold rod (99.99%) with diameter 6 mm and height 6 mm was purchased from Alfa Aesar (Johnson Matthey, Ward Hill, MA).

Femtosecond Laser Ablation. Laser ablation was carried out with a Ti/sapphire laser (Hurricane, Spectra Physics Lasers, Mountain View, CA), which provided 110 fs full width at half-maximum (fwhm) pulses (wavelength 800 nm, maximum energy 1 mJ/pulse, repetition rate of 1 kHz). The radiation was focused by an objective with the focal distance 7.5 cm onto a gold target, which was placed on the bottom of a 3-mL glass vessel filled with aqueous solutions of cyclodextrins (Figure 1). The depth of the liquid layer above the rod was about 12 mm.

Measurements. UV–vis measurements were performed using a spectrophotometer (DU-640, Beckman, CA) and room temperature in the range 300 – 800 nm with a 1-cm optimal length cuvette. A transmission electron microscope (TEM Philips CM30, Philips, FEI, Hillsboro, OR) with 0.23 nm point–point resolution was used to take the electron images of the

[†] Ecole Polytechnique de Montreal.

[‡] Steacie Institute of Molecular Sciences, National Research Council Canada.

[§] Biotechnology Research Institute, National Research Council Canada.

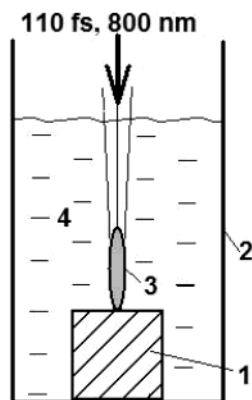


Figure 1. Experimental setup: 1, gold target; 2, glass vessel; 3, plasma plume; 4, aqueous solution.

nanoparticles in the solution. A drop of a sample solution was placed on a carbon-coated copper grid and dried at room temperature. The grid was washed with deionized water to remove unbound CDs. Typically, the diameters of 500–1000 particles in sight of a given micrograph were measured and the distribution of particle size (diameter) was calculated. In addition, craters on the target surface were also observed by scanning electron microscopy (SEM, Phillips XL20, FEI, Hillsboro, OR) and a profilometer (Dektak 3030, Veeco, Santa Barbara, CA). Solution-phase FT-Raman spectra were recorded using a Bruker FRA 106 spectrometer (Bruker Optics, Milton, ON, Canada) equipped with a liquid nitrogen-cooled germanium detector and a 1064 nm Nd:YAG laser. Samples were mounted inside the instrument using a 0.5 cm quartz cuvette with a mirrored rear surface. The Raman spectrum was collected within the 0–4000 cm^{-1} interval with 4 cm^{-1} resolution using 500 mW of excitation laser power. The CD–gold colloids were examined with a triple-quadrupole mass spectrometer (API III LC/MS/MS, Sciex, Thornhill, ON, Canada) to monitor the degradation of CD if any during the course of femtosecond laser ablation. Charged ions were generated by spraying the sample solution through a stainless steel capillary held at 4–6 kV, and the sample solution was delivered to the sprayer by a syringe infusion pump through a fused silica capillary of 100 μm i.d. A gas curtain formed by a continuous flow (0.6–1.8 L/min) of N_2 in the interface region served to evaporate the aerosol droplets and to break up the cluster formation from supersonic expansion. The potential on the sampling orifice of the instrument was set at +30 V.

Results and Discussion

Ablation in Pure Water. We used a femtosecond laser technique, which was anticipated to minimize the average particle size and narrow the size distribution of ablated particles due to both a relatively low ablation threshold and the absence of target heating effects.⁶ In pure deionized water, the ablation led to visible changes of the solution color after only several seconds in the experiment. Optical absorption spectra of gold colloids exhibited the characteristic peak of the surface plasmon resonance at 520–540 nm, similar to those obtained with Sigma gold nanoparticles. TEM micrographs revealed that most of the particles had sizes of 40–60 nm; however, a rather broad size distribution ranging from 25 to 120 nm was observed (Figure 2). The height and the width of the SPR peak at 520 nm were dependent upon the energy of the laser pulses. At 0.16 mJ/pulse the height and width at 520 nm were lower and less broadened in comparison to the case of the ablation performed at 0.8 mJ/

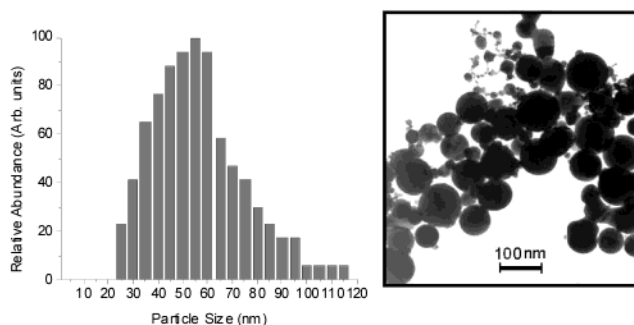


Figure 2. TEM micrograph image (right) and corresponding size distribution (left) of gold particles prepared by femtosecond laser ablation in deionized water.

pulse. Measuring the diameter of the ablated crater on a target by SEM and a profilometer, and its depth by profilometer (Dektak 3030, Veeco), we were able to determine the volume of ablated gold per pulse. The estimated volume values for 0.8 and 0.16 mJ/pulse were $(7-8) \times 10^{-11} \text{ cm}^3$ and $(1-3) \times 10^{-11} \text{ cm}^3$, respectively. This was consistent with the results of Mafune et al.,^{7b} who have shown that the nanoparticles can only be produced above a threshold laser power and that their number density increases proportionally with the laser power. It should be noted that a 532-nm Nd:YAG laser^{5d,7b} had significantly larger energy per pulse (90 mJ/pulse), which should influence the absolute abundance of the produced particles.

The mechanism of laser ablation could be explained in terms of the dynamic formation mechanism postulated by Mafune and co-workers.¹⁰ In brief, a dense cloud of gold atoms (plume) was accumulated in the laser spot of the gold target during the course of ablation. This core was made of a number of small gold atoms that were aggregated accidentally due to the density fluctuation to form embryonic nanoparticles. Even when the ablation process had been terminated, the aggregation continued at a significantly slower growth rate until all atoms in the vicinity (~ 40 nm) of the embryonic nanoparticles were depleted.¹⁰ As both ablated atoms and embryonic nanoparticles diffuse through the solution toward each other to form larger clusters, this consecutive nanoparticle growth was slow, random, and uncontrollable.

Ablation in Aqueous Cyclodextrin Solutions. We were able to effectively ablate the gold target in aqueous solutions of CDs. Ablation in the presence of all three CDs led to a deep red solution, as reflected by a strong absorption band at 520 nm. However, the increase of the CD concentration was accompanied by a certain decrease of the red color intensity. This was especially noticeable for 10 mM β -CD or γ -CD, which had only a weak pink color. It should be noted that the absorption spectra obtained for the Sigma particles (5-, 10-, and 20-nm diameter) indicated that the 520-nm peak height was dependent on the total particle density and the particle size. Therefore, the absorption spectra alone could not be used to estimate the total particle concentration formed during ablation. TEM micrographs revealed that the nanoparticles were nearly spherical and their average sizes decreased with an increase in the CD concentration with a very sharp particle size distribution (Figure 3). Chemical analysis indicated that not even traces of glucose, a possible major degradable product of CDs, was present in the solution. Mass spectrometric data also confirmed that the gold colloids prepared in α -, β -, and γ -CD, respectively, still exhibited molecular masses of 972, 1135, and 1297, the molecular weights of the three CD molecules, and no other peaks were recorded. In view of such data, CDs were considered intact during the course of ablation. The preparation of CD-modified gold

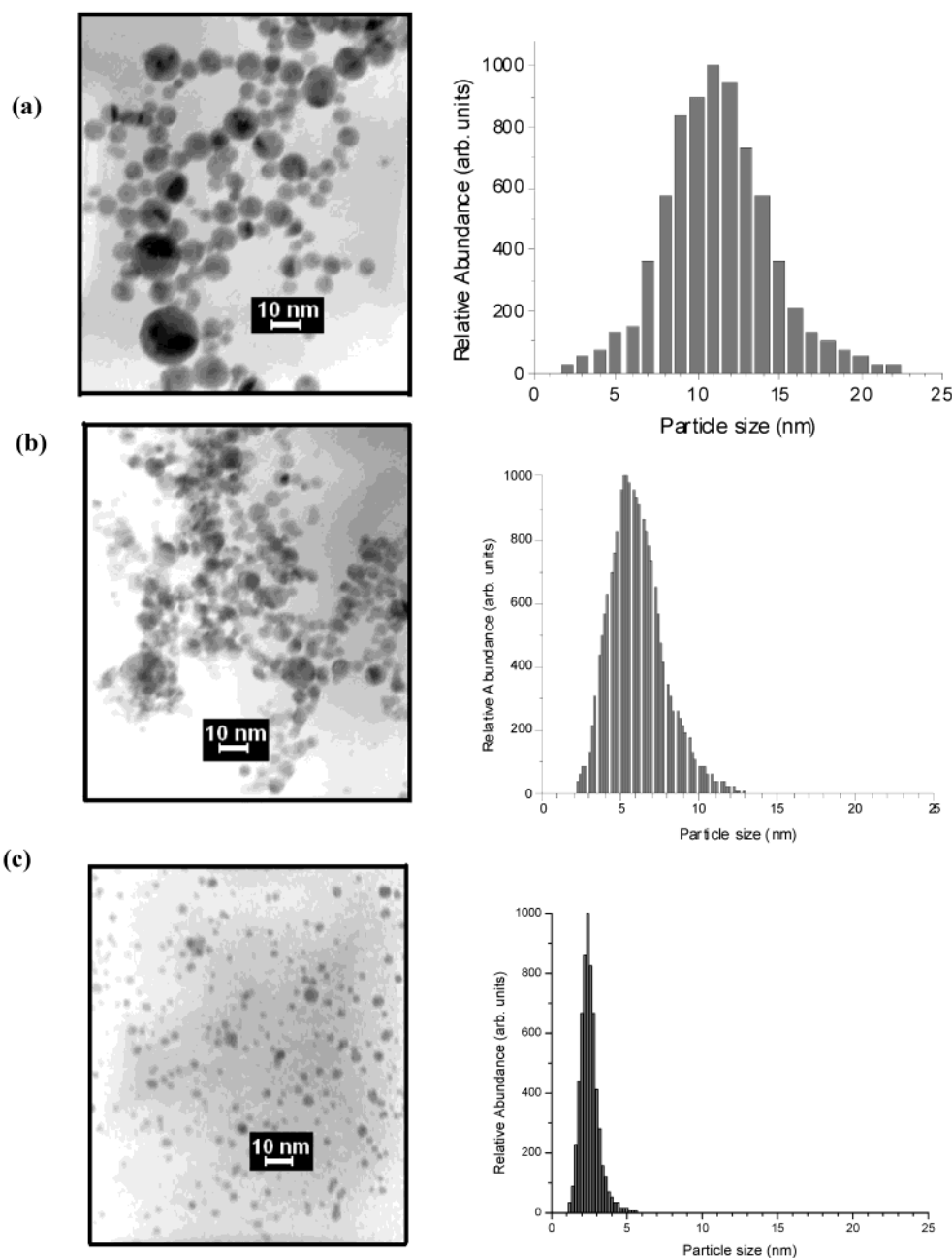


Figure 3. TEM micrograph image and corresponding size distribution of gold particles prepared by femtosecond laser ablation in (a) 0.1 mM β -CD, (b) 1 mM β -CD, and (c) 10 mM β -CD. The laser energy was 0.8 J/pulse.

nanospheres by Rojas et al.⁹ by chemical reduction did not report any concern related to CD degradation.

β -CD was most effective in reducing the size and dispersion of the gold nanoparticles, followed by γ -CD and α -CD. Ablation in 10 mM β -CD produced particles with the average size 2.1–2.3 nm (Figure 4, top) with a size dispersion less than 1 nm fwhm (Figure 4, bottom). It should be noted that the laser ablation in the presence of 100 mM SDS led to much larger 4.6–8 nm particles with the dispersion of 5 nm fwhm.^{7a,10} In addition, the surface of gold nanoparticles would be completely covered by SDS, which renders such particles hardly useful for chemical modifications or sensing applications. From the reduction of AuCl_4^- in the presence of perthiolated CD receptors, the nature of the perthiolated CD (α , β , or γ) was also reported to affect the average particle size ranging from 2 to 7 nm.¹¹

Stability of Gold Colloids. In pure water, the absorbance measured at 520 nm retained only 7% of its original value after

5 days of aging in ambient conditions. Several precipitates were observed in the storage glass vial, and the solution became dark blue, which confirmed that the nanoparticles continued to grow and/or aggregate with time in the solution. In contrast, gold colloids prepared in the presence of CDs exhibited good stability. In β -CD (0.1–10 mM), the 520-nm peak height remained constant within this time window. The corresponding values for α -CD and γ -CD were 70% and 60%, respectively. Indeed, nanoclusters of β -CD remained well dispersed in 10 mM β -CD for over 45 days with minimal loss of absorption intensity (5–7%). This was very encouraging, since all of the experiments were performed without any precaution taken, such as oxygen-free conditions or use of protective agents, except for CDs.

Postulated Mechanism of the CD Effect. As a subject of ongoing research in our laboratory, a mechanism for the formation and/or stabilization of the gold nanoparticles by CDs has not been understood. However, it was evident that CDs

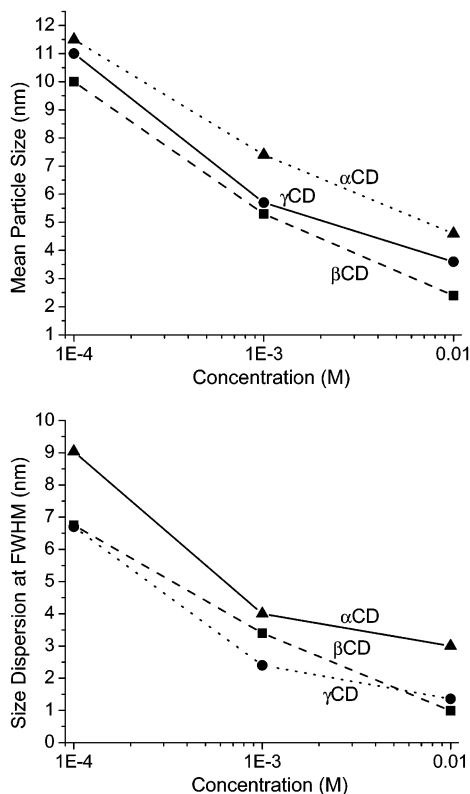


Figure 4. Effect of the CD concentration on the resulting average particle size (top) and the size dispersion at fwhm (bottom).

played a critical role in controlling the size as well as the stability of gold nanoparticles. The apolar cavity of the three CDs (internal diameter of 570, 780, and 950 pm, respectively) has been known to form inclusion complexes with various small hydrophobic molecules.⁸ With such a dimension, a single and hydrophobic gold atom (288 pm in diameter) and/or small gold nanoclusters would be enclosed in the CD cavity to form an inclusion complex. Indeed, it has been reported that the apolar rhodium nanoparticles are stabilized by hydrophobic cavities of a number of the CDs.¹²

FT-Raman measurements were taken in an attempt to probe possible gold–CD interactions. Spectra were recorded for the three 10 mM CD stock solutions and the corresponding colloidal gold solutions. Figure 5 shows the results obtained for the pair of β -CD samples. A small but reproducible reduction in intensity of the low-frequency β -CD modes was observed following the production of gold nanoparticles (see inset Figure 5). Explanations such as concentration differences or inconsistent sample preparation are unlikely, since all other features of the Raman spectra are identical. The effected modes correspond to pyranose ring vibrations along the backbone of the CD.¹³ Dampening of these modes suggests an interaction between gold and the primary macrocyclic structure of the CD. This is consistent with the proposed mechanism that single or small numbers of gold atoms are held within the hydrophobic cavity of the CD, removing them as an available feedstock for nanoparticle growth. The magnitude of the observed intensity reduction is not surprising considering the large excess of β -CD compared to the concentration of gold particles. An identical dampening effect was observed in the Raman spectra of the α -CD stock and colloidal gold solutions, but no dampening was observed in the pair of γ -CD spectra. γ -CD possesses the largest internal cavity diameter of the three. Gold atoms included within the γ -CD cavity should be less-strongly coupled to the γ -CD

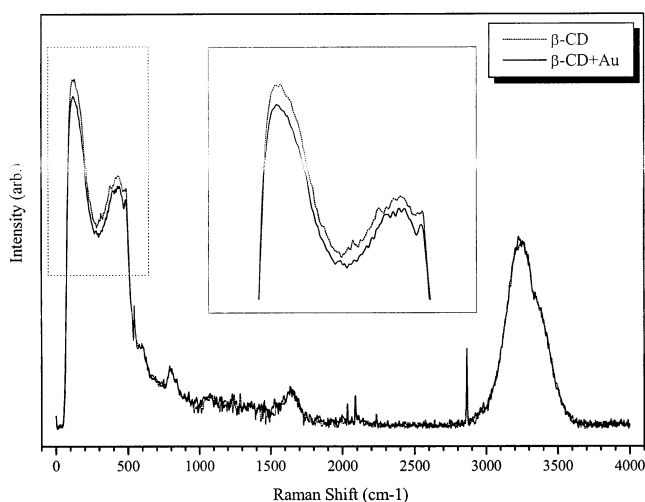


Figure 5. FT-Raman spectra of a 10 mM β -CD stock solution (dotted line) and colloidal gold nanoparticles in 10 mM β -CD (solid line). The inset highlights the dampening effect on the low-frequency β -CD vibrational modes due to the presence of gold. Sharp features are laser artifacts.

backbone, making any interactions difficult to observe over the large background of “free” γ -CDs in solution. No evidence of Au–O interactions can be obtained from the Raman spectra.

The resulting nanoparticles were much smaller and more stable with increase in the CD concentration, implying that hydrophobic interactions between gold nanoparticles and CD molecules were of sufficient strength to prevent agglomeration, as demonstrated by TEM and UV–vis absorption spectroscopy. Consequently, embryonic nanoparticles formed in the plume became limited and had to compete with CD molecules for free ablated gold atoms in the vicinity of this region through diffusion. As CDs could form stable inclusion complexes with free ablated atoms and small nanoparticles as well as exhibit hydrophobic interactions with embryonic nanoparticles, the consecutive particle growth due to the mutual coalescence between such objects was severely limited or terminated, particularly at high CD concentrations. This hypothesis was partly supported by the experimental data to confirm that the nanoparticle size and dispersion decreased with increasing CD concentrations. With the lowest aqueous solubility (18.5 g/L), β -CD should exhibit the strongest hydrophobic interaction with gold compared to those of both α - (145 g/L) and γ -CD (232 g/L).⁸ Because both ablation and the formation of inclusion complexes between CD molecules and developing Au particles took place almost simultaneously, the interplay between the kinetics of the two processes was likely the key factor that governed the average size diameter of the gold nanoparticles. Unlike resorcinarenes,¹⁴ there was no evidence to suggest that CD molecules were capable of binding to ablated atoms by chemisorption through Au–O interactions. This point was taken into account, since there are 18, 21, and 24 hydroxyl groups for α -, β -, and γ -CD, respectively.⁸

Conclusion

Many of the chemical methods involve the use of toxic chemicals and might give rise to toxic side products. In this study, laser ablation has been proven as an environmentally friendly procedure for fabricating monodispersed gold nanoparticles and gold colloid was very stable in high CD concentrations. The laser ablation method can be applied at ambient conditions with no disturbing chemical impurities introduced.

This is reproducible, and the reduction is initiated homogeneously; that is, there are no local concentration gradients when reactants are mixed, as encountered in chemical reduction. Polymers in small concentration, such as polyphosphate, polyacrylate, poly(vinyl sulfate), poly(vinyl alcohol), and poly(ethyleneimine), are often used to stabilize the growing aggregates.^{1a} Very recently, surfactants such as resorcinarenes¹⁴ and SDS^{5d,10} have been used to stabilize gold nanoclusters. To our knowledge, CDs have not been used for size control and stabilization of gold nanoparticles. This CD-mediated size control is a promising technique and can be extended for fabrication of other metal nanoparticles, and work is in progress toward this objective.

Acknowledgment. The authors thank Dr. E. Sacher and Mr. J.-P. Sylvestre of Ecole Polytechnique for several useful discussions and NSERC Canada for financial assistance.

References and Notes

- (1) (a) Henglein, A. *J. Phys. Chem.* **1993**, *97*, 5457. (b) Link, S.; El-Sayed, M. A. *J. Phys. Chem. B* **1999**, *103*, 4212. (c) Link, S.; El-Sayed, M. A. *J. Phys. Chem. B* **1999**, *103*, 8410. (d) Hodak, J. H.; Martini, I.; Hartland, G. V.; Link, S.; El-Sayed, M. A. *J. Chem. Phys.* **1999**, *108*, 9210.
- (2) (a) Takagi, M. *J. Phys. Soc. Jpn.* **1954**, *9*, 359. (b) Buffat, D. A.; Borel, J. P. *Phys. Rev.* **1976**, *A13*, 2289. (c) Haruta, M. *Catal. Today* **1997**, *36*, 153.
- (3) (a) Hirai, H.; Wakabayashi, H.; Komiyama, M. *Chem. Lett.* **1983**, 1047. (b) Lisiecki, I.; Pileni, M. P. *J. Am. Chem. Soc.* **1993**, *115*, 3887. (c) Ahmadi, T. S.; Wang, Z. L.; Green, T. C.; Hendlein, A.; El-Sayed, M. A. *Science* **1996**, *272*, 1924. (d) Huang, H. H.; Yan, F. Q.; Kek, Y. M.; Chew, C. H.; Xu, G. Q.; Ji, W.; Oh, P. S.; Tang, S. H. *Langmuir* **1997**, *13*, 172.
- (4) Petit, C.; Lixon, P.; Pileni, M. P. *J. Phys. Chem.* **1993**, *97*, 12974.
- (5) (a) Fojtik, A.; Henglein, A. *Ber. Bunsen-Ges. Phys. Chem.* **1993**, *97*, 252. (b) Sibbald, M. S.; Chumanov, G.; Cotton, T. M. *J. Phys. Chem.* **1996**, *100*, 4672. (c) Yeh, M. S.; Yang, Y. S.; Lee, Y. P.; Lee, H. F.; Yeh, Y. H.; Yeh, C. S. *J. Phys. Chem.* **1999**, *103*, 6851. (d) Mafune, F.; Kohno, J.-Y.; Takeda, Y.; Kondow, T.; Sawabe, H. *J. Phys. Chem.* **2000**, *104*, 8333.
- (6) *LIA Handbook of Laser Materials Processing*; Ready, J. F., Farson, D. F., Eds.; Springer-Verlag and Heidelberg GmbH & Co.: Berlin, 2001; pp 499–508.
- (7) (a) Mafune, F.; Kohno, J.-Y.; Takeda, Y.; Kondow, T.; Sawabe, H. *J. Phys. Chem.* **2001**, *105*, 9050. (b) Mafune, F.; Kohno, J.-Y.; Takeda, Y.; Kondow, T. *J. Phys. Chem. B* **2002**, *106*, 8555. (c) Mafune, F.; Kohno, J.-Y.; Takeda, Y.; Kondow, T.; Sawabe, H. *J. Phys. Chem. B* **2000**, *104*, 9111. (d) Mafune, F.; Kohno, J.-Y.; Takeda, Y.; Kondow, T. *J. Phys. Chem. B* **2002**, *106*, 8555.
- (8) Szejtli, J. In *Comprehensive Supramolecular Chemistry*; Atwood, J. L., Davies, J. E. D., Macnicol, D. D., Vogtle, F., Eds.; Pergamon-Elsevier: New York, 1996; Vol. 3, pp 5–40.
- (9) Rojas, M. T.; Koniger, R.; Stoddart, J. F.; Kaifer, A. E. *J. Am. Chem. Soc.* **1995**, *117*, 336.
- (10) Mafune, F.; Kohno, J.-Y.; Takeda, Y.; Kondow, T.; Sawabe, H. *J. Phys. Chem. B* **2001**, *105*, 5144.
- (11) Liu, J.; Ong, W.; Roman, E.; Lynn, M. J.; Kaifer, A. E. *Langmuir* **2000**, *16*, 3000.
- (12) Komiyama, M.; Hirai, H. *Bull. Chem. Soc. Jpn.* **1983**, *56*, 2883.
- (13) Wiedenhof, J. N.; Lammers, J. J.; Van Panthaleon, C. L.; Van Eck, B. *Die Stärke* **1969**, *21*, 119.
- (14) Stavens, K. B.; Pusztay, S. V.; Zou, S.; Andres, R. P.; Wei, A. *Langmuir* **1999**, *15*, 24.